Journal of Catalysis 285 (2012) 1–5

Contents lists available at SciVerse ScienceDirect

Journal of Catalysis

journal homepage: www.elsevier.com/locate/jcat

Priority Communication

Unprecedented selectivity to the direct desulfurization (DDS) pathway in a highly active FeNi bimetallic phosphide catalyst

S. Ted Oyama [a,b,*], Haiyan Zhao [a], Hans-Joachim Freund [c], Kiyotaka Asakura [d,e], Radosław Włodarczyk [f], Marek Sierka [f]

[a] Department of Chemical Systems Engineering, The University of Tokyo, 7-3-1 Hongo, Bunkyo-ku, Tokyo 113-8656, Japan
[b] Department of Chemical Engineering, Virginia Tech, Blacksburg, VA 24061, USA
[c] Department of Chemical Physics, Fritz Haber Institute of the Max Planck Society, Faradayweg 4-6, Berlin 14195, Germany
[d] Catalysis Research Center, Hokkaido University, Kita 21-10, Sapporo 001-0021, Japan
[e] Department of Quantum Science and Technology, Hokkaido University, Kita 21-10, Sapporo 001-0021, Japan
[f] Institut für Chemie, Humboldt-Universität zu Berlin, Unter den Linden 6, 10099 Berlin, Germany

ARTICLE INFO

Article history:
Received 8 May 2011
Revised 29 June 2011
Accepted 8 August 2011
Available online 22 October 2011

Keywords:
NiFeP
Deep HDS
DFT
EXAFS
Nickel iron phosphide
4,6-Dimethyldibenzothiophene

ABSTRACT

The hydrodesulfurization (HDS) of the refractory compound 4,6-dimethyldibenzothiophene (DMDBT) normally proceeds through a hydrogenation pathway that removes the planarity of the ring system and makes the hindered sulfur atom more accessible to the desulfurization centers. In this study, a highly active dispersed bimetallic NiFeP catalyst is found to have high selectivity for a direct desulfurization pathway, which does not require prior hydrogenation. The compound has equal numbers of Ni and Fe atoms which extended X-ray absorption fine structure analysis indicates are distributed randomly in the hexagonal Fe_2P structure, with just a slight enrichment of Fe on the surface. This is supported by density functional theory calculations. The remarkable properties of the catalyst are ascribed to a ligand effect of Fe on the active Ni atoms.

1. Introduction

Reduction of the sulfur content in transportation fuels is an area of great current activity in the refining industry [1]. Recent reviews describe conventional hydroprocessing and emerging processes such as oxidative desulfurization and biodesulfurization [2,3]. Conventional hydroprocessing is challenging because it requires the hydrodesulfurization (HDS) of refractory compounds such as 4,6-dimethyldibenzothiophene (4,6-DMDBT), in which the sulfur is sterically protected [4]. Sulfur removal on commercial promoted catalysts such as CoMo or NiMo sulfides proceeds by a hydrogenation (HYD) route in which the 4,6-DMDBT is partly hydrogenated to render the molecule non-planar and the sulfur accessible to the catalyst surface [5]. Here, we report a bimetallic NiFe phosphide catalyst, which has higher activity than commercial catalysts, and which follows a direct desulfurization (DDS) route that allows removal of the sulfur without prior hydrogenation (Scheme 1a). This has been long a goal in the field because it permits HDS to be carried out with less consumption of expensive hydrogen while retaining valuable high-octane aromatics in the product. Analysis of the bimetallic catalyst by X-ray absorption fine structure (EXAFS) reveals that it exposes low-coordination sites that are particularly active for DDS. Density functional theory (DFT) calculations provide information on the site occupancy in the alloy. We anticipate that these findings will lead to the exploration of other phosphide catalysts with structures that can be modified and controlled by alloying.

Early work [6,7] showed that the HDS activity of common phosphides follows the order: Ni_2P > WP > MoP > CoP > Fe_2P. A number of bimetallic phosphides such as Ni_xMo_yP [8,9], Co_xMo_yP [10,11], and Ni_xCo_yP [12,13] have also been studied because a synergistic effect between the components was foreseen as found for promoted metal sulfides. Unexpectedly, however, these bimetallic phosphide phases did not show enhanced activity or selectivity over the component Ni, Co, or Mo phosphides, except for the case of an unsupported [10] and supported [13] $Co_{0.08}Ni_2P$ where respective increases in conversion over Ni_2P of 67% were found in the HDS of 4,6-DMDBT and 34% in the HDS of thiophene. Recently, studies with unsupported and silica-supported $Fe_xNi_{2-x}P_y$ catalysts [14] showed a modest 10% activity increase in the HDS of dibenzothiophene with a Ni-rich catalyst ($x = 0.03$). In this study, we explore the activity of similar $FeNiP/SiO_2$ catalysts for the deep HDS of 4,6-DMDBT.

* Corresponding author at: Department of Chemical Systems Engineering, The University of Tokyo, 7-3-1 Hongo, Bunkyo-ku, Tokyo 113-8656, Japan.
E-mail address: oyama@vt.edu (S. Ted Oyama).

0021-9517/$ - see front matter © 2011 Elsevier Inc. All rights reserved.
doi:10.1016/j.jcat.2011.08.006

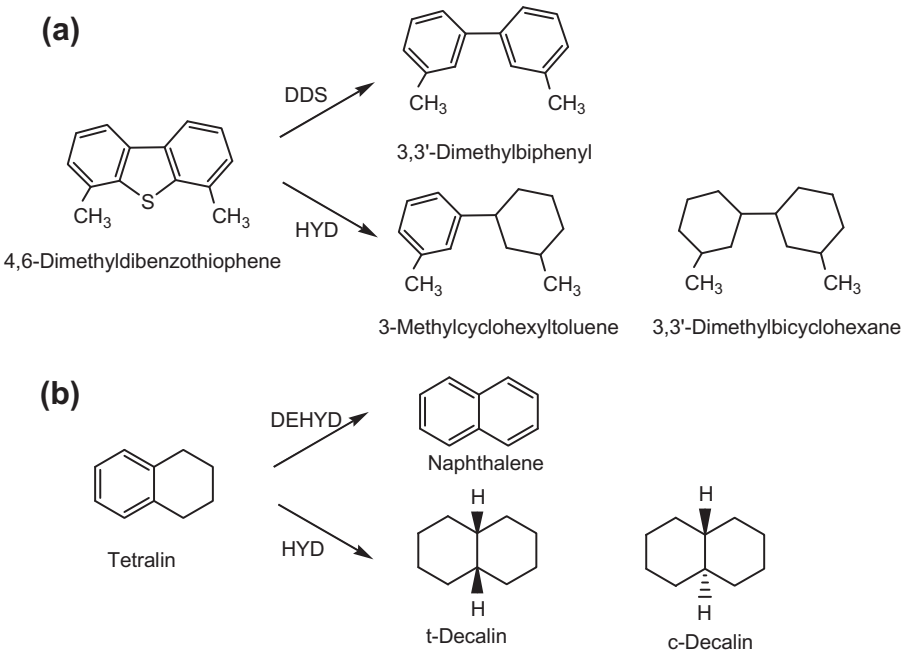

Scheme 1. (a) Products of 4,6-dimethyldibenzothiophene desulfurization, (b) products of tetralin dehydrogenation and hydrogenation.

2. Methods

The compounds Ni_2P/SiO_2, NiFeP(3:1)/SiO_2, NiFeP(1:1)/SiO_2, and Fe_2P/SiO_2 were prepared where the numbers in parenthesis are molar ratios. The synthesis involved temperature-programmed reduction (TPR), following procedures reported previously [15,16]. Briefly, the synthesis involved impregnation of metal phosphate precursors on a silica support (Cabosil EH5), followed by reduction to the phosphides at ~560 °C. The total metal molar loading was 1.6 mmol g^{-1} (mmol per g of support) in all cases. The proportion of metals in the precursors were in the stoichiometric ratios indicated above, but the phosphorus content was quadrupled because earlier work had shown that this produced active compositions in the case of Ni_2P [16].

The activity of the catalysts for 4,6-DMDBT HDS was compared at 340 °C and 30 bar [6,7] with a H_2 flow rate of 150 cm^3(NTP)/min and a contact time of 2.4 s. Quantities of catalysts loaded in the reactor corresponded to the same amount of CO or atomic oxygen uptake (240 μmol) and were 2.18 g for the Ni_2P/SiO_2, 2.50 g for the NiFeP(3:1)/SiO_2 catalyst, 4.00 g for the NiFeP(1:1)/SiO_2 catalyst, 4.62 g for the Fe_2P/SiO_2, and 1.26 g for the Ni–Mo–S/Al_2O_3 catalyst. Note that the Ni–Mo–S catalysts are an optimized commercial catalyst with very high dispersion. The use of CO chemisorption to count the surface metal sites in phosphides is reasonable. Early studies comparing unsupported and supported materials indicated that the same turnover frequencies were obtained when CO was used as a probe [6,17]. The use of O_2 chemisorption to titrate sites in sulfides serves only as an approximation [18], but it has been shown that pulse chemisorption at dry ice/acetone temperatures avoids corrosive chemisorption [19,20], and this method was used here.

X-ray absorption spectra at the Ni K-edge (8.333 keV) and Fe K-edge (7.112 keV) of reference and catalyst samples were recorded in the energy range 8.233–9.283 keV at beam line X18B at the National Synchrotron Light Source at Brookhaven National Laboratory. Measurements were taken by standard absorption methods on samples loaded in cells with Kapton windows without exposure to the atmosphere. The EXAFS data were analyzed by the program REX [21,22]. Phase shift and amplitude functions were derived from the FEFF8 program [23].

Hydrotreating activities of the samples were measured in a three-phase, packed-bed reactor operated at 30 bar and 340 °C with a model feed liquid containing 500 ppm sulfur as 4,6-DMDBT, 3000 ppm sulfur as dimethyl disulfide, 200 ppm nitrogen as quinoline, 1 wt.% tetralin, 0.5 wt.% n-octane as internal standard, and balance n-tridecane.

Periodic density functional theory (DFT) calculations were carried out using the Vienna Ab Initio Simulation package (VASP) [24] and the Perdew, Burke and Ernzerhof (PBE) exchange–correlation functional [25]. The calculations were performed using the projector augmented wave method (PAW) [26]. Only the valence electrons were explicitly considered. Optimizations of cell parameters used a $7 \times 7 \times 13$ Monkhorst–Pack k-point mesh [27]for the Brillouin-zone sampling and an energy cutoff of 1000 eV for a plane wave basis set. The Pulay stress arising from the incomplete basis set was minimized by restarting the optimization until self-consistency of the total energy was reached. Optimizations of atomic positions were performed with a $4 \times 4 \times 7$ Monkhorst–Pack k-point mesh and a plane wave cutoff of 400 eV. $1 \times 1 \times 2$ supercells was used for calculations of electronic density of states (DOS).

3. Results and discussion

The high activity of Ni_2P has prompted many studies of its synthesis, structure and reactivity [28]. The crystal structure [29]of Ni_2P is hexagonal (a_o = 0.5859 nm, c_o = 0.3382 nm) with space group $p\bar{6}2m$ where the metal atoms are of two types, M(1) at position 3(f) with tetrahedral coordination and M(2) at position 3(g) with square pyramidal coordination (Fig. 1). From the average of M–P bond distances, the size of the M(1) site can be calculated to be 0.223 nm and that of the M(2) site 0.243 nm, so the M(1) site is smaller. A recent study [30] showed that the M(1) site carries out DDS while the pyramidal M(2) site is particularly active for HYD and that the latter is exposed on small Ni_2P crystallites. It was of interest to study NiFeP because Fe_2P is isostructural with Ni_2P [31,32] and substitution of Fe for Ni was surmised to change the electronic properties of the cluster. From the structure [33] of Fe_2P (a_o = 0.5865 nm, c_o = 0.3456 nm), the size of the M(1) site is 0.225 nm and that of the M(2) site is 0.246 nm.

The following series of compounds were tested: Ni_2P/SiO_2, NiFeP(3:1)/SiO_2, NiFeP(1:1)/SiO_2, and Fe_2P/SiO_2. The Ni_2P showed

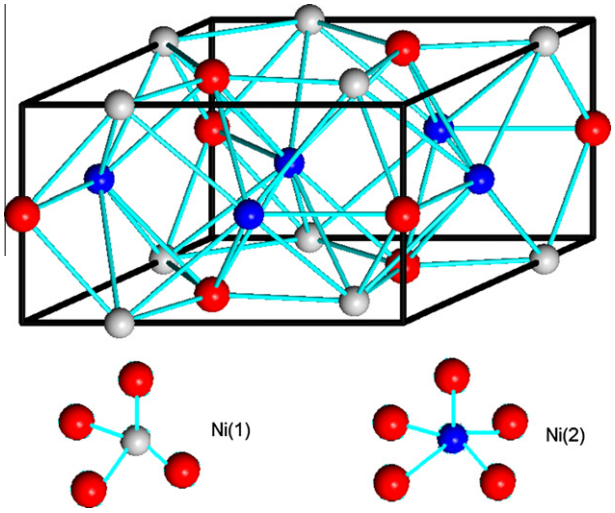

Fig. 1. Crystal structure of Ni_2P showing tetrahedral M(1) and square pyramidal M(2) sites.

the highest HDS conversion (99%), while the catalysts containing increasing amounts of Fe showed slightly lower activity while the Fe_2P catalyst was essentially inactive, as found earlier for dibenzothiophene HDS [16]. The selectivity results at steady state showed remarkable dependency on composition (Fig. 2). Whereas the Ni_2P/SiO_2 had a DDS selectivity of only 12%, the samples with Ni/Fe ratio of 3:1 and 1:1 showed increasing DDS selectivity of 70% and 85%. These high values for DDS are unprecedented in the hydrotreating literature where typical selectivity for a CoMo catalyst is ~30% and for a NiMo catalyst is ~20% in the HDS of 4,6-DMDBT at similar conditions [34]. The results are particularly notable as the high DDS selectivity is obtained at high conversion, which would tend to favor the HYD products. In contrast to these compounds, the Fe_2P/SiO_2 had very low activity, as also found previously [14]. This is not surprising, among sulfides iron [35] and iron alloys [36] are among the least active compositions.

To rule out that the observed selectivity to DDS products could be due to the secondary dehydrogenation of the HYD products, experiments were conducted with a cofeed of tetralin, which can undergo dehydrogenation to naphthalene or hydrogenation to decalin (Scheme 1b). The experimental conditions were the same as for

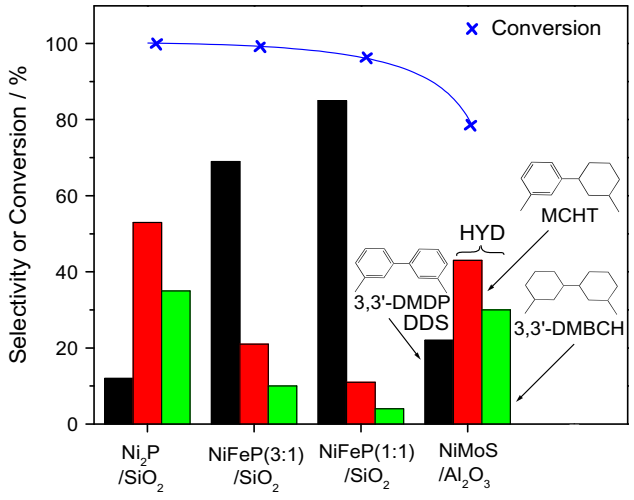

Fig. 2. Steady-state reactivity of $NiFeP/SiO_2$ samples and reference sulfide at 340 °C and 30 bar.

the HDS reaction, except that 10% tetralin was added and the solvent reduced accordingly. It was found that the conversion of tetralin was 26% and the selectivities were 25% naphthalene, 49% trans-decalin, and 26% cis-decalin. If dehydrogenation were the thermodynamically preferred reaction at the reaction conditions, then tetralin should produce naphthalene. In fact naphthalene was the minority product. The experiment demonstrates directly that the selectivity to the diphenyl is kinetically controlled even at close to 100% HDS conversion, and this is supported by thermodynamic calculations [28]. The DDS products are kinetically favored because the sulfur compounds are adsorbed strongly on the surface and prevent hydrogenation of the primary aromatic products. Note that the tetralin level was substantially higher than the 4,6-DMDBT (10,000 ppm vs. 500 ppm) in the above measurements.

Density functional theory calculations (DFT) were undertaken to shed light on the bulk electronic structure of the materials. The calculated structural parameters for Ni_2P (a_o = 0.5886 nm, c_o = 0.3372 nm) and Fe_2P (a_o = 0.5809, c_o = 0.3428 nm) show less than 1% deviation from the experimental [29,33] data. Calculations on the FeNiP structures containing 100% Fe and 100% Ni in M(1) sites, respectively, indicate only a 1.30 kJ mol^{-1} of metal sites preference for Fe occupation of M(1) sites. This minute energetic difference shows that M(1) and M(2) sites could be occupied by both Ni and Fe. Indeed, additional calculations performed for different FeNiP structures containing 67%, 50%, as well as 33% Fe in M(1) sites confirm that configurations with mixed M(1) and M(2) occupations are the most stable. Electronic density of states of FeNiP (Not shown) clearly indicates changes in the metallic nature of this alloy compared to the pure Fe_2P and Ni_2P compounds, which both also reveal metallic character [37,38].

Recent characterization of $Fe_xNi_{2-x}P_y$ catalysts with Mössbauer effect spectroscopy [14] indeed confirms that for x = 1, the M(1) sites are occupied by both Fe and Ni atoms (about 67% Ni and 33% Fe). The experiments also indirectly confirm the small energy differences between different occupation patterns since the fraction of Fe atoms that occupy M(1) site is not constant, but smoothly changes with respect to the composition of catalyst. Thus, for low Ni contents (x > 0.60), the Ni atoms preferentially occupy M(1) sites, but for high Ni contents (x < 0.60), this site preference is reversed, and Ni atoms preferentially occupy M(2) sites.

To obtain further insight on the materials, the $NiFeP(1:1)/SiO_2$, which showed the highest selectivity for DDS products, was characterized by X-ray absorption fine structure (EXAFS) spectroscopy. Analysis was carried out with a two-shell model for comparison between the samples of different composition. Earlier work used a three-shell analysis, which explicitly accounted for M(1) and M(2) contributions [30], but this was not considered appropriate with the current multi-element data. Comparison was made with Ni_2P/SiO_2 and Fe_2P/SiO_2. The results (Table 2) are consistent with the known structure of the compounds. The bond distances in Ni_2P are smaller than those of Fe_2P, in agreement with the crystallographic results. For NiFeP, fits were made with Ni in the M(1) sites, Fe in the M(1) sites and 50–50 mixtures, and only the latter gave a good agreement with the experimentally determined spectra (Fig. 3). With this, the bond distances in the NiFeP compound were obtained and found to be in between those of Ni_2P and Fe_2P. The coordination numbers in the compounds are lower than the average bulk M–P and M–M coordinations of 5 and 8, consistent with the small particle size determined by X-ray line broadening (Table 1).

Examination of the details (Table 2) allows a number of observations. First, it is noted that the metal–phosphorus (M–P) and metal–metal (M–M) distances are larger in Fe_2P than in Ni_2P, consistent with the known lattice spacings (Table 1). Second, in the NiFeP material, the Ni–P and Fe–P distances of 0.218 and 0.216 nm are close, as are the Ni–M and Fe–M distances of 0.261 and 0.265 nm,

Table 2
X-ray absorption fine structure parameters for NiFeP (1:1)/SiO_2.

Sample	Bond pair	CN[a]	Distance (nm)	Debye–Waller factor (nm)
Ni_2P/SiO_2	Ni–P	1.8(2)	0.218(3)	0.0077(2)
	Ni–Ni	3.2(5)	0.260(3)	0.0092(3)
Fe_2P/SiO_2	Fe–P	2.3(2)	0.221(3)	0.0092(2)
	Fe–Fe	1.9(7)	0.268(3)	0.0083(3)
NiFeP (1:1)/SiO_2	Ni–P	1.9(2)	0.218(3)	0.0091(2)
	Ni–Ni (or Ni–Fe)	4.3(5)	0.261(4)	0.0088(3)
	Fe–P	1.7(2)	0.216(3)	0.0089(2)
	Fe–Fe (or Fe–Ni)	1.9(7)	0.265(3)	0.0080(3)

[a] Coordination number. The values in parenthesis show the error in the last digit.

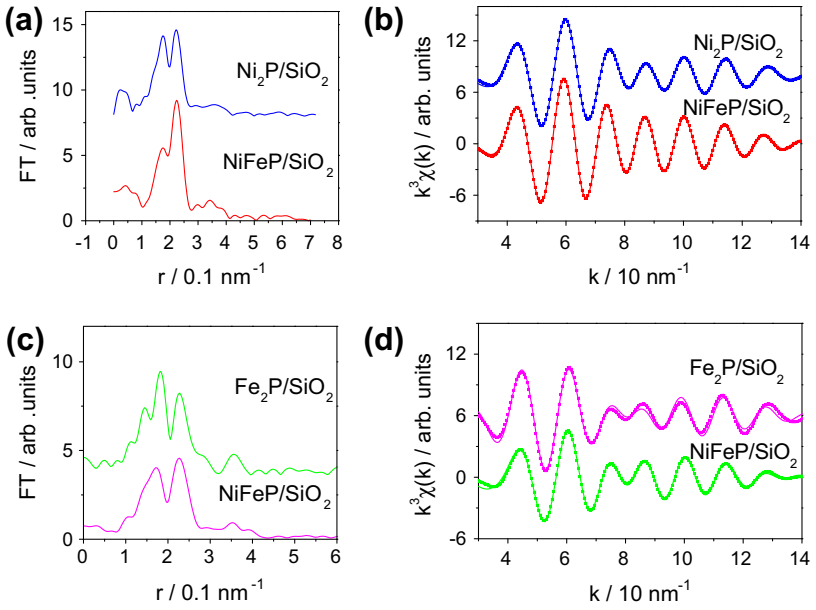

Fig. 3. EXAFS data of Ni_2P, Fe_2P, and NiFeP (1:1)/SiO_2, (a) magnitude of the Fourier transform of the Ni K-edge spectra, (b) Ni K-edge EXAFS spectra (points) and model (line) from NiFeP/SiO_2, (c) magnitude of the Fourier transform of the Fe K-edge spectra, (d) Fe K-edge EXAFS spectra (points) and model (line) NiFeP/SiO_2.

so that the Fe and Ni atoms likely occupy sites interchangeably in the structure. This agrees with the DFT results. Third, the Ni–P and Fe–P distances are short, 0.218 and 0.216 nm, and correspond to distances expected for a metal in the tetrahedral M(1) site (0.22 nm) rather than the pyramidal M(2) site (0.24 nm). Fourth, the coordination numbers of the Fe–P and Fe–M bonds (1.7 and 1.9) are smaller than those of the Ni–P and Ni–M bonds (1.9 and 4.3).

There are two different interpretations for the third observation of short Ni–P and Fe–P distances. Interpretation (a): The EXAFS intensity for a collection of distances around a scattering atom will be stronger for the shorter distances [39] so in this case, EXAFS is probing just the M(1) site, with average M–P distance of 0.223 nm, rather than the M(2) site with average M–P distance of 0.243 nm. Thus, it can say little about the relative numbers of M(1) and M(2) sites. Interpretation (b): The EXAFS intensity can have contributions from both M(1) and M(2) sites, and the short distance indicates an organization of the structure that makes M(1) sites more numerous.

There are also two interpretations for the fourth observation about the lower coordination numbers associated with the Fe atoms in comparison with the Ni atoms. (c) The Fe is preferentially, though not exclusively, located at the surface, where nearest neighbor numbers are smaller. (d) Fe prefers M(1) sites that have lower coordination (4) than M(2) sites (5). Taking possibilities a and c in combination gives a first model of the NiFeP catalyst as consisting of the hexagonal $p\bar{6}2m$ structure (Fig. 1) with mostly random occupation of the M(1) and M(2) sites but with Fe in a slight excess at the surface in either of these sites. Taking possibilities b, c, and d in combination gives a second model of the catalyst in which the hexagonal NiFeP nanoparticles are terminated by M(1) sites that are slightly more occupied by Fe atoms than Ni atoms. This is because in the bulk material, there should be an equal numbers of M(1) sites and M(2) sites, and the excess M(1) sites would only be possible if the nanoparticles were terminated by these sites. The DFT calculations are consistent with both structures.

The special reactivity of the FeNi bimetallic phosphide can be understood from either structural model as revealed by EXAFS. In

Table 1
Characterization of NiFeP/SiO_2 samples.

Sample	Surface area ($m^2\ g^{-1}$)	CO uptake ($\mu mol\ g^{-1}$)	Particle size,[a] nm (±2 nm)
Ni_2P/SiO_2	135	110	10
NiFeP(3:1)/SiO_2	138	96	7
NiFeP(1:1)/SiO_2	153	60	9
Fe_2P/SiO_2	148	52	5
NiMoS/Al_2O_3	160	95[b]	N/D

N/D: Not determined.
[a] From Scherrer equation.
[b] O_2 Uptake.

the first model, which has both Ni and Fe on the surface, the catalytic activity is attributed to the Ni atoms, as Fe_2P is inactive. The special reactivity of the bimetallic material is probably due to a ligand effect of Fe on Ni, which must also account for the high selectivity to DDS. In the second model, the activity is again ascribed to the Ni atoms, with the high activity again due to a ligand effect. However, the presence of the M(1) sites on the surface have been associated with the DDS reaction on Ni_2P nanoparticles [30], and their presence on the surface of the bimetallic NiFeP nanoparticles could account for the observed selectivity. The M(1) sites are only fourfold coordinate and so are more accessible to the hindered sulfur atom in 4,6-DMDBT. Although DFT calculations suggested that the M(1) sites are more preferable on the surface of $Ni_2P(0001)$ [40], it should be noted that previous work on Ni_2P/SiO_2 proposed that M(2) sites are found on the surface of small particles [30]. The recent work with Mössbauer effect spectroscopy cited earlier [14] finds that a $Fe_{0.03}$–$Ni_{1.97}P_{2.00}/SiO_2$ catalyst had a thiophene HDS activity 40% higher than an optimized 25 wt.% $Ni_{2.00}P_{1.60}/SiO_2$ catalyst (at 370 °C) and suggested that Ni in M(2) sites (about 70%) is present on the surface of this low Fe content sample. For a FeNi(1:1) composition, the entire sample contains only about 22% Ni in M(2) sites, so at the surface, it may be that the presence of Fe makes Ni prefer M(1) sites, contrary to what is found in pure Ni_2P/SiO_2. More work is necessary to clarify this. It should also be noted that past studies have indicated that the active phase is a phosphosulfide [41–43]. Indeed, EXAFS examination of the catalyst after reaction, a detailed description of which is beyond the scope of this paper, reveals the presence of sulfur in quantities less than a monolayer. So the description of the sites above must encompass the presence of sulfur at reaction conditions. Regardless of the interpretation, the activity results are remarkable and the possibility of ligand effects with metals other than Fe presents a unique opportunity to design new improved catalysts.

Acknowledgments

We acknowledge support from the US Department of Energy, Office of Basic Energy Sciences, through Grant DE-FG02-963414669, the National Renewable Energy Laboratory through Grant DE-FG3608GO18214, the Humboldt Foundation for a Senior Research Award to STO, and the Japan Ministry of Agriculture, Forestry, and Fisheries (Norinsuisansho). RW and MS acknowledge support from the Deutsche Forschungsgemeinschaft (Cluster of Excellence "Unifying Concepts in Catalysis").

References

[1] R.G. Leliveld, S.E. Eijsbouts, Catal. Today 130 (2008) 183.
[2] A. Stanislaus, A. Marafi, M.S. Rana, Catal. Today 153 (2010) 1.
[3] S.T. Oyama, T. Gott, H. Zhao, Y.K. Lee, Catal. Today 143 (2009) 94.
[4] T.C. Ho, Catal. Today 98 (2004) 3.
[5] T. Kabe, A. Ishihara, Q. Zhang, Appl. Catal. A: Gen. 97 (1993) L1.
[6] X. Wang, Y.K. Lee, W.J. Chun, S.T. Oyama, F. Requejo, J. Catal. 210 (2002) 207.
[7] P. Clark, X. Wang, S.T. Oyama, J. Catal. 207 (2002) 256.
[8] F. Sun, W. Wu, Z. Wu, J. Guo, Z. Wei, Y. Yang, Z. Jiang, F. Tian, C. Li, J. Catal. 228 (2004) 298.
[9] J.A. Rodriguez, J.-Y. Kim, J.C. Hanson, S.J. Sawhill, M.E. Bussell, J. Phys. Chem. B 107 (2003) 6276.
[10] I.I. Abu, K.J. Smith, J. Catal. 241 (2006) 356.
[11] V. Zuzaniuk, R. Prins, J. Catal. 219 (2003) 85.
[12] I.I. Abu, K.J. Smith, Appl. Catal. A: Gen. 328 (2007) 58.
[13] A.W. Burns, A.F. Gaudette, M.E. Bussell, J. Catal. 260 (2008) 262.
[14] A.F. Gaudette, A.W. Burns, J.R. Hayes, M.C. Smith, R.H. Bowker, T. Seda, M.E. Bussell, J. Catal. 272 (2010) 18.
[15] J.F. Deng, H. Li, W. Wang, Catal. Today 51 (1999) 113.
[16] X. Wang, P. Clark, S.T. Oyama, J. Catal. 208 (2002) 321.
[17] P.A. Clark, S.T. Oyama, J. Catal. 218 (2003) 78.
[18] S.J. Tauster, T.A. Pecoraro, R.R. Chianelli, J. Catal. 63 (1980) 515.
[19] W. Zmierczak, G. MuraliDhar, F.E. Massoth, J. Catal. 77 (1982) 432.
[20] T.A. Bodrero, C.H. Bartholomew, K.C. Pratt, J. Catal. 78 (1982) 253.
[21] T. Taguchi, AIP Conf. Proc. 882 (2007) 162.
[22] K. Asakura, in: Y. Iwasawa (Ed.), X-ray Absorption Fine Structure for Catalysts and Surfaces, World Scientific, Singapore, 1996, pp. 33–58.
[23] J.J. Rehr, J.J. Kas, M.P. Prange, A.P. Sorini, Y. Takimoto, F. Vila, CR Phys. 10 (2009) 548.
[24] G. Kresse, J. Furthmüller, Phys. Rev. B 54 (1996) 11169.
[25] J.P. Perdew, K. Burke, M. Ernzerhof, Phys. Rev. Lett. 78 (1997) 1396.
[26] G. Kresse, D. Joubert, Phys. Rev. B 59 (1999) 1758.
[27] H.J. Monkhorst, J.D. Pack, Phys. Rev. B 13 (1976) 5188.
[28] Y. Shu, Y.K. Lee, S.T. Oyama, J. Catal. 236 (2005) 112.
[29] S. Rundqvist, Acta Chem. Scand. 16 (1962) 992.
[30] S.T. Oyama, Y.K. Lee, J. Catal. 258 (2008) 393.
[31] J.B. Goodenough, J. Appl. Phys. 40 (1969) 1250.
[32] J.P. Sénateur, A. Rouault, P. L'Héritier, A. Krumbügel-Nylund, R. Fruchart, D. Fruchart, P. Convert, E. Roudaut, Mater. Res. Bull. 8 (1973) 229.
[33] S. Rundqvist, F. Jellinek, Acta Chem. Scand. 13 (1959) 425.
[34] J.H. Kim, X. Ma, C. Song, Y.-K. Lee, S.T. Oyama, Energy Fuels 19 (2005) 353.
[35] T.A. Pecoraro, R.R. Chianelli, J. Catal. 67 (1981) 430.
[36] T.C. Ho, Catal. Today 130 (2008) 206.
[37] F. Luo, H.-L. Su, W. Song, Z.-M. Wang, Z.-G. Yan, Ch.-H. Yan, J. Mater. Chem. 14 (2004) 111.
[38] K. Edamoto, Y. Nakadai, H. Inomata, K. Ozawa, S. Otani, Solid State Commun. 148 (2008) 135.
[39] E.D. Crozier, J.J. Rehr, R. Ingalls, in: D.C. Koningsberger, R. Prins (Eds.), EXAFS, XANES and SEXAFS, Wiley, New York, 1988.
[40] P. Liu, J.A. Rodriguez, T. Asakura, J. Gomes, K. Nakamura, J. Phys. Chem. 109 (2005) 4575.
[41] S.T. Oyama, X. Wang, Y.-K. Lee, W.-J. Chun, J. Catal. 221 (2004) 263–273.
[42] T. Kawai, K.K. Bando, Y.-K. Lee, S.T. Oyama, W.-J. Chun, K. Asakura, J. Catal. 241 (2006) 20.
[43] A.E. Nelson, M. Sun, A.S.M. Junaid, J. Catal. 241 (2006) 180.